AIAA JOURNAL
Vol. 44, No. 9, September 2006

Nonlinear Response of Highly Flexible Structures to Air Blast Loads: Application Shelters

Hitesh Kapoor,* Sangeon Chun,† Rakesh K. Kapania,‡ Michael R. Motley,§ and Raymond H. Plaut¶
Virginia Polytechnic Institute and State University, Blacksburg, Virginia 24061

The dynamic response of flexible membrane structures to blast loads is described, with application toward shelter systems. Shelters such as the Tent Extendable Modular Personnel tents fall into the category of highly flexible membrane structures due to their large deformation behavior. Material testing was conducted to determine the material properties of the liner and the canvas material. A finite element model for the shelter structure was developed, and the dynamic response to blast loading conditions was obtained. Transient analysis was performed based on an implicit approach in which the time integration was done using the Newmark method, and the Newton–Raphson method was used for the nonlinear analysis. Dynamic responses consisting of displacement time histories and dynamic stresses were computed for the membrane model. A parametric study was performed, and design recommendations are presented.

I. Introduction

FLEXIBLE structures, due to being lightweight and having multifunctional capabilities and low cost, are widely used in many engineering fields such as the aerospace, civil, and automotive industries. Communication antennas, solar thermal propulsion systems, space solar power units, and solar sails are examples of flexible aerospace structures. Gossamer spacecraft[1] are large-apertured, highly integrated, thin-walled structures with multiple functional capabilities and are modeled as flexible membrane structures. In civil engineering, some exhibition pavilions, storage facilities, tents, and domes are classical examples of flexible membrane structures. Automotive air bags, hot-air balloons, airships, large sandbags for flood protection, flexible tanks, and storage vessels are constructed from high-strength fabrics. In marine conditions, membrane structures find usage as breakwaters, fluid-filled airbags, and sea balloons.

A shelter basically consists of a fabric skin supported over a frame structure. Applications for military and civilian purposes include expeditionary shelters such as Tent Extendable Modular Personnel (TEMPER) tents and small shelter systems,[2] U.S. Army chemical protection medical systems, collective protection systems[3] for protection against chemical and biological agents, U.S. Army's expandable light air mobility shelters,[4] and accordion expandable shelter (AES) rapid deployment shelters. Such structures may be used as temporary housing for people, maintenance hangers in aviation, emergency shelters, and mobile field hospitals.

The U.S. Army has been involved in the development of lightweight shelters consisting of a fabric skin supported by pressurized arches. The arches are made of a thin flexible material and take a very stiff structural form when inflated, providing the framework for the shelter system. Mohan and Kapania[5] studied the behavior of these arches under snow and wind loads. Mohan considered a tent consisting of a membrane skin connected to inflated arches and analyzed the large-deformation behavior using a three-node, flat, triangular element, combining the discrete Kirchhoff theory plate bending element and a membrane element similar to the Allman element. Mohan and Kapania included the follower effect of the pressure load and observed that it enhances the convergence of the solution. Carradine and Plaut[6] performed an experimental study on arch-supported membrane structures under snow and wind loads, using scale models. It was concluded that the failure mode for the membrane was tearing occurring near connections of the skin to the frame.

The response of these and similar soft structures to blast and impact loads has generated much interest with the idea of their utilization in combat zones, where they are subjected to projectiles and exploding bombs. Shelters such as TEMPER tents (Fig. 1)[2] are used for various field applications by the U.S. Air Force. TEMPER tents consist of a fabric skin supported over a metal frame with a slightly pressurized collective protection system (CPS) M28 (Ref. 7) liner attached inside the frame. Presently, these kinds of structural systems are being tested for the force protection standards against explosions at some distance from the structure. In field tests carried out by the U.S. Air Force Research Laboratory,[2] it was revealed that the liner was damaged due to the air-blast explosion, with major damage comprising tearing of the liner on the back side of the tent (Fig. 2).[2] This paper details computational modeling of such structural systems. The present research analyzes the material behavior of the liner system through material testing and deals with the complete finite element model development of TEMPER tents and their structural response under highly dynamic conditions generated by blast loads.

In general, the response of structures to dynamic loading is very difficult to predict due to the dependence on multiple factors such as the duration of the loading, peak load, shape of the pulse, impulse energy, boundary conditions, and nonlinear material, and geometric behavior. Turkmen[8] studied the structural response of isotropic plates to blast loads. The plate was modeled using shell elements, and an implicit approach was used for the transient solution. It was observed that, due to the presence of geometric nonlinearities, significant membrane strain occurred. Gupta et al.[9] examined the elastoplastic dynamic response of rectangular plates due to blast loading. It was observed that the peak displacement for the nonlinear geometric model was reached earlier in time than in the linear model and that it was smaller.

Koh et al.[10] studied the response of shell structures to blast loads with applications such as blast-resistant doors. The skin was modeled with shell elements, and the edge stiffeners were modeled with

Presented as Paper 2005-2030 at the AIAA/ASME/ASCE/AHS/ASC 46th Structures, Structural Dynamics, and Materials Conference, Austin, TX, 18–21 April 2005; received 28 June 2005; revision received 21 November 2005; accepted for publication 22 November 2005.

*M.S. Graduate Student, Department of Aerospace and Ocean Engineering. Member AIAA.
†Postdoctoral Fellow, Department of Aerospace and Ocean Engineering. Member AIAA.
‡Professor, Department of Aerospace and Ocean Engineering. Associate Fellow AIAA.
§Graduate Assistant, Department of Civil and Environmental Engineering; currently Design Engineer, The LPA Group, Inc., Tallahassee, FL 32301.
¶D. H. Pletta Professor of Engineering, Department of Civil and Environmental Engineering.

Fig. 1 TEMPER tent overview and internal liner (CPS).

Fig. 2 Blast damage to TEMPER tent liner on back side.

beam elements. The maximum displacement occurred over the skin away from the stiffeners. Louca and Pan[11] considered the dynamic response of stiffened and unstiffened plates under blast loads. Explicit codes DYNA-3D and ABAQUS/Explicit were used to simulate the response of the plate, modeled using shell elements.

Lightweight barriers form an effective part of some protection systems developed to guard against explosions. High ratios of allowable strain to stress and allowable stress to density, and smaller spans, are the most desired characteristics sought when considering a light barrier. Scherbatiuk[12] studied the effects of such barriers on the transmission of blast waves. The barrier was modeled with the membrane and bending effects combined, membrane only, bending only, and a moving rigid-wall formulation to determine their effects on the transmission of blast. Crawford and Morrill[13] studied such barrier designs consisting of a screen supported over a frame with cable anchorage to support the barrier. Zhu[14] examined an optical technique for obtaining the dynamic response experimentally and compared the results with a numerical solution. He used the variational finite difference approach for the elastoplastic response of a clamped rectangular plate under impact and pressure loading. Experimental tests predicted that the plate initially took the shape of a flat plateau and with time the plateau contracted toward the center and formed a pyramidlike permanently deformed shape.

Turkmen[15] examined the behavior of composite laminated structures to blast loads. A finite element solution was obtained using a shell-based model. It was observed that larger moduli resulted in smaller peak values but higher-frequency response. Niyogi et al.[16] analyzed vibration of the laminated folded plate structures. These structures, due to their high-strength, low weight, and high stiffness, are used for various engineering applications. Chen et al.[17] developed the finite strip method for the nonlinear transient analysis of composite plates. The transient analysis for isotropic, orthotropic, and laminated plate models was performed under blast loads, and the central plate deflections and stress time histories were plotted. Membrane behavior is often characterized by large deformations. Jenkins and Leonard[18] reviewed the dynamic response associated with membrane structures. Smalley et al.[19] studied the structural modeling of a 5-m thin-film inflatable structure. Approaches generally used to obtain converged solutions for such cases involve either adding an arbitrary stiffness term or using an artificial constraint to aid convergence.

The present work uses the literature review in understanding the behavior of similar-type tent structures to other types of loads. The literature review on response of shell structures to blast loading condition is also useful. The present research extends previous work to the blast response of highly flexible tent structures, consisting of a fabric skin connected to a frame. Literature on such structures is not readily available. Material testing was conducted to determine the material properties of the liner and canvas material. Finite element models for the shelter structure were developed using ANSYS 8.0. Static analysis was carried out for increasing transverse pressure loading, and membrane-dominated behavior was observed. Stresses were obtained for both the outer skin (canvas) and liner material. Transient analysis was performed based on an implicit approach, where time integration was done using the Newmark method and the Newton–Raphson method was used for the nonlinear analysis. Responses consisting of displacement time histories and stresses were computed. A parametric study was carried out, and design considerations are discussed.

II. Material Testing

Because of the special nature of the liner material, tests were conducted to determine its material properties. Tension tests were run using an Instron machine on strips measuring 2.54 cm in width. The liner was measured to be 0.31 mm thick. The orthotropic M28 material consists of a woven layer that is laminated with a thin plastic sheet. The strips were oriented with the edges of the squares parallel to the edges of the strips (square-oriented strips) and then with the squares skewed to roughly a 45-deg angle with the edges (diamond-oriented strips), as shown in Fig. 3. Young's modulus was in the range of 625–775 MPa for the first case, whereas the modulus for the diamond-oriented strips was less than one-half of that. The failure stresses for the square-oriented strips were in the range of 35–50 MPa, whereas those for the diamond-oriented strips were 30–40 MPa. To gather a more accurate assessment of the failure stress of larger sheets of the liner, grab tests were run on 10.2-cm-wide sheets of the liner. The response was nonlinear, and failure occurred in the sheets at tension forces around 1000 N. To be conservative, the values for maximum failure stress and Young's modulus

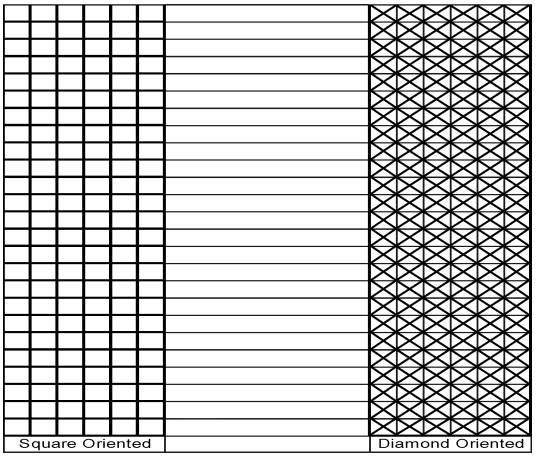

Fig. 3 Square-oriented and diamond-oriented 2.54-cm-wide strips.

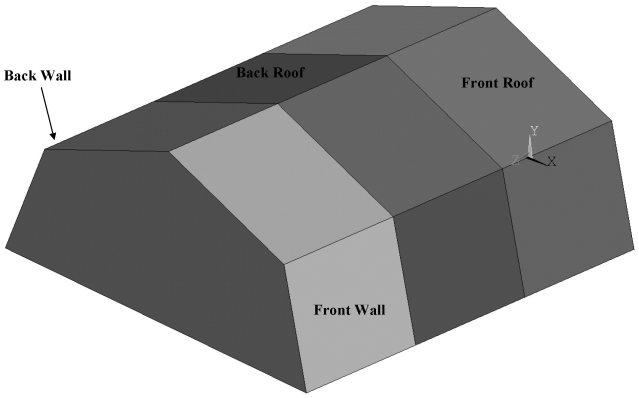

Fig. 4 Tent model front and back sides.

were taken from the tests on the diamond-oriented strips. Young's modulus for the canvas was found to be between 35 and 42 MPa. Failure stresses for the majority of the specimens were between 15 and 20 MPa. This is much less than the failure stresses exhibited by the liner. However, the difference in thickness (with the canvas just over twice the thickness of the liner) leads to the fact that the failure load is close for the two materials in similar strips.

III. Finite Element Modeling

TEMPER tents consist of a fabric skin supported over an aluminum frame fitted with the CPS M28 (Ref. 7) liner and a ventilation system that provides clean air to the closed liner and maintains a positive pressure inside the liner slightly above the surrounding atmospheric pressure. This positive pressure ensures that the flow of air is outward from the liner, thus not allowing contaminated air to enter. Each transverse frame structure is separated from adjacent ones by 2.43 m (8 ft) and interconnected by aluminum rods. The thickness of the fabric skin is 0.65 mm (0.0255 in.). The tent consists of four sides, front wall, front roof, back wall, and back roof, where the front denotes the blast-facing side. A simplified finite element model[20] consisting of the fabric skin (modeled using shell elements) connected to the frame structure (modeled using beam elements) was developed using ANSYS.[21] Three finite element models are considered, using different element types and element formulations. This section details the finite element models. Figure 4 shows the tent model.

A. Shell Kinematics

The problem involves a structure with thickness smaller by several orders compared to the other dimensions. It has been observed that it is difficult to comprehend shell behavior as the thickness is reduced, and therefore, it is essential to determine the sensitivity of the structure to variations in thickness. This discussion is based on the investigation of Lee and Bathe[22] on the asymptotic behavior[23] of shell structures. They[22] found that the behavior of a shell converges to a specific limit state (zero-displacement state) as the thickness approaches zero.

Shell kinematics consists of bending, membrane, and shearing actions as the basic loading mechanisms. These states correspond to bending, membrane, and shear strain energy states. Because the thickness is very small, the shear energy state is negligible. Shell problems are, therefore, referred to as bending-dominated, membrane-dominated, or mixed. A bending-dominated state is referred to when the shell carries load by the bending action, whereas in a membrane-dominated state, the load is carried by the membrane action. The mixed action is referred to when the bending and membrane actions act in combination to control the behavior of the shell. When large deformations are included, a pure bending state is seldom encountered because membrane stresses are generated. Because of these large deformations, initially shells carry load in both membrane and bending action, but with time the characteristic changes to purely membrane-dominated behavior. An important aspect of the structural analysis of membranes, regardless of the membrane thickness, is that significant bending develops near restraints. The presence of this bending could result in numerical problems if appropriate care is not taken in the numerical simulation.

B. Drill Degree of Freedom

A separate nodal coordinate system (or nodal triad) is introduced at the element nodal level to restrain the computational degrees of freedom. For flat shell elements, this corresponds to the original nodal triad in the global system. In the flat shell formulation for curved structures, each element generates the nodal surface normals at the shared nodes. These surface normals[24] are used to define the averaged surface normal vectors. If coplanarity exists between the elements, these normals are identical, resulting in rank deficiency in the assembled matrix. The drill freedom is not resisted here, thus, resulting in a singularity in the global matrix. This problem is more pronounced in folded plate models and can be eliminated by suppressing the drill degree of freedom.

The drill degree of freedom[24] is defined as the rotational degree of freedom normal to the plane of the element and is denoted by θ_z, assuming that the surface normal is the local z direction. In most of the formulations, this does not form part of the membrane kinematics of the shell. The absence of this drill freedom causes rank deficiency.

Two basic approaches are implemented. First, an artificial drill stiffness parameter is used to remove the rank deficiency for those elements without drill freedom. This artificial stiffness parameter acts as a spring stiffness for the sixth degree of freedom, θ_z. An inappropriate value of this parameter can affect the solution dramatically. One technique is to give a large value for this parameter; this acts as a penalty parameter and causes the computed solution for the drill degree of freedom to be nearly zero. Therefore, it is important to determine the nodal points that need to be penalty imposed; for example, at a stiffener–skin interaction, the drill freedom of the stiffener element is the bending rotation and there is no need to impose the penalty. However, if all of the elements meeting at a node are coplanar, there is a need to add a penalty to avoid the singularity. This situation arises for folded plate segments and at the straight boundaries of developable surfaces (e.g., cylinders or cones).

Alternatively, a small value may be specified, and thus, its contribution to the strain energy will be nearly zero regardless of the solution obtained for the drill degree of freedom. This approach deals with the removal of rank deficiency or singularity without influencing the finite element approximation for the element and leads to a perfectly well-behaved set of equations from which all of the displacements can be obtained. The generalized coordinate θ_z does not affect the stresses and is uncoupled from all of the equilibrium equations. Application of this approach brings programming complexities; therefore, modifications are required so that the rotational parameters arise more naturally and have real physical meaning. This can be accomplished by introducing a rotational degree

of freedom in the membrane kinematics. Element formulations are available that inherently possess the drill freedom and, thus, do not exhibit rank deficiency or a singularity.

C. Model 1

For model 1, the fabric skin is modeled using shell 63 elements and the frames using beam 4 elements.[21] Shell 63 has six degrees of freedom at each node: translations in the nodal x, y, and z directions and rotations about the nodal x, y, and z axes. It allows for both membrane-bending and membrane-only (neglecting bending stiffness) options. It includes stress stiffening and large-deflection capabilities and provides a consistent tangent stiffness matrix option for use in large-deflection (finite rotation) analysis. This consistent tangent stiffness matrix is derived from the discretized finite element equilibrium equations without the introduction of various approximations. The use of a consistent tangent stiffness in a nonlinear analysis increases the rate of convergence greatly. It normally results in a quadratic rate of convergence. Inclusion of the Allman rotational stiffness option for in-plane rotational stiffness enhances the convergence behavior in large-deflection analysis of planar shell structures (flat shells, or flat regions of shells). Figure 5 shows the finite element model for the shelter. Triangular elements are used.

D. Model 2

Here, the fabric skin is modeled using shell 181 elements and the frames with beam 4 elements.[21] Shell 181 is suitable for analyzing thin to moderately thick shell structures. It is a four-node element with six degrees of freedom at each node. If the membrane-only option is used, the element has translational degrees of freedom only. Shell 181 is well suited for nonlinear applications and accounts for follower (pressure load stiffness) effects of distributed pressures. This feature helps in accelerating the convergence of the solution and is essential for large-deformation behavior. Shell 181 uses a penalty method to relate the independent rotational degrees of freedom about the normal to the shell surface with the in-plane components of displacements. The ANSYS program chooses an appropriate penalty stiffness by default. User input is allowed through the real constant input. Figure 6 shows the finite element model for the shelter using shell 181 elements.

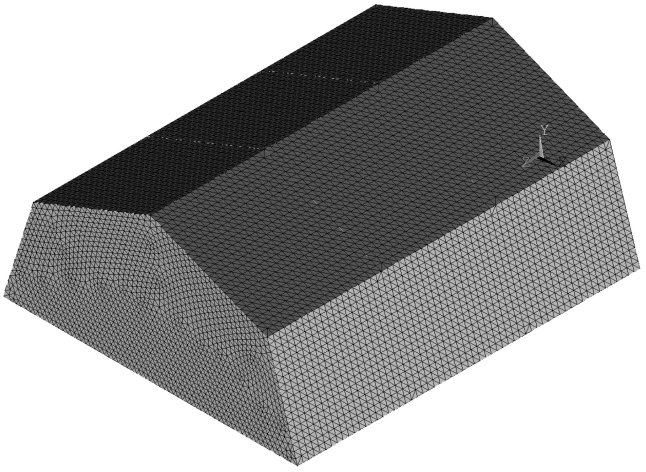

Fig. 5 Finite element model/shell 63.

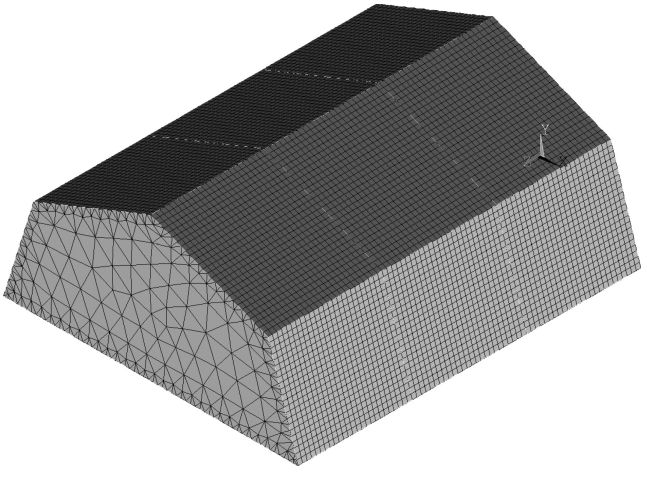

Fig. 6 Finite element model/shell 181.

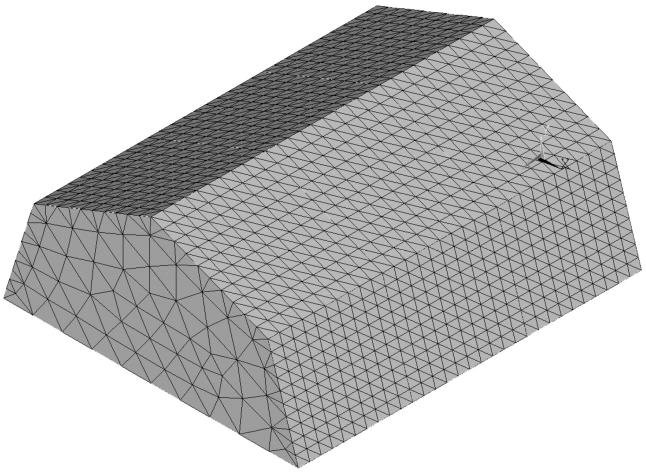

Fig. 7 Finite element model/shell 41.

E. Model 3

For model 3, the skin is modeled with shell 41 (membrane-only) elements and the frames are modeled with beam elements, using the assumption that stress couples are neglected over the whole region. Shell 41 is a three-dimensional element[21] having membrane (in-plane) stiffness but no bending (out-of-plane) stiffness, intended for shell structures where bending of the elements is of secondary importance. The element has three degrees of freedom at each node: translations in the nodal x, y, and z directions. It includes stress stiffening and large-deflection options. The out-of-planenature within the element, or roundoff error in nodal locations, may cause instability in the displacement solution. To counteract this, the element has the option of adding a slight normal stiffness with the elastic foundation stiffness parameter, which has been used to avoid any convergence problems. Figure 7 shows the finite element model for the tent using shell 41 elements.

IV. Nonlinear Static Analysis

The static analysis is performed for a clamped plate model under pressure loads for canvas and liner material models. The analysis takes into account the large-deformation behavior. A small value of elastic foundation stiffness (to avoid out-of-planeness) is added to enhance the convergence. For the nonlinear solution, the Newton–Raphson method with line search is used to obtain the converged solution. The stress stiffening effects are included while performing the analysis, which plays an important role in a thin structure's analysis. Stress stiffening (also called geometric stiffening) is the stiffening of a structure due to its stress state. This stiffening effect normally needs to be considered for thin structures with very small bending stiffness compared to transverse stiffness resulting from in-plane stresses, such as cables, thin beams, and shells (membranes) and couples the in-plane and transverse displacements. This effect also augments the regular nonlinear stiffness matrix produced by large-strain or large-deflection effects.

A. Case 1

Static analysis for a square plate under clamped conditions is performed. The t/a ratio is 0.00065, where t is the thickness of the plate and a is the width. The material model is elastic with $E = 35$ MPa and $\nu = 0.3$. Shell 63 (elastic shell element) and shell 41 are used

to simulate the static response. Nonlinear static analysis of a square plate under uniformly distributed pressure load of magnitude P_0 is performed. Figure 8 shows the deformation profiles for Shell 63 for pressure loads ranging from 5000 to 30,000 Pa. Figure 9 shows the nonlinear response of the shell structure as the pressure is increased. The deformation increases, and the structure behaves more and more like a membrane. Element types shell 63 and shell 41 are compared and found to behave similarly. Von-Mises stresses are computed and found to increase with the increasing pressure loads (see Ref. 25).

B. Case 2

Here, a static analysis is performed for the liner material. A clamped square plate is considered. The t/a ratio is 0.00031 and $a = 1$ m. The elastic properties $E = 670$ MPa and $\nu = 0.3$ are used. Nonlinear static analysis of the square plate under a uniformly distributed pressure load of magnitude P_0 is performed. Figure 10 shows the nonlinear response. As the pressure load is increased, deformation increases and the structure carries load more and more in membrane action. When the deformation is compared with that obtained in case 1 for a given pressure load, the maximum displacement is reduced due to transverse stiffening of the plate. The stresses are increased significantly compared to those in case 1 (Ref. 25).

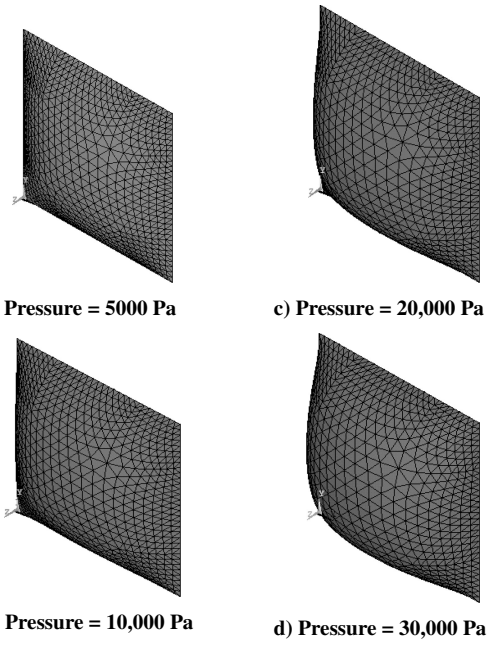

Fig. 8 Displacement profile of plate using shell 63 under uniform pressure load.

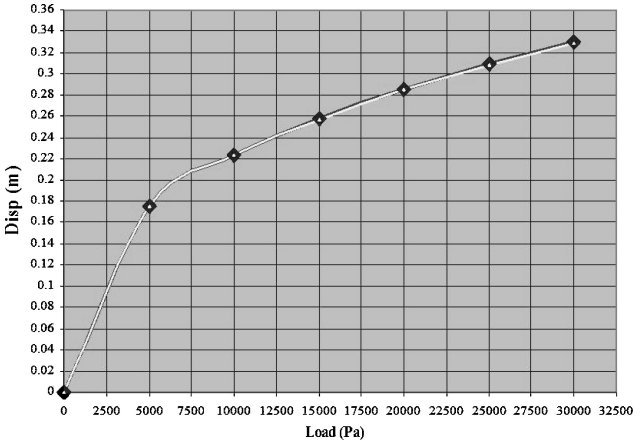

Fig. 9 Plate nonlinear response: maximum transverse displacement with increasing pressure loading using shell 63 (upper line) and shell 41 (lower line).

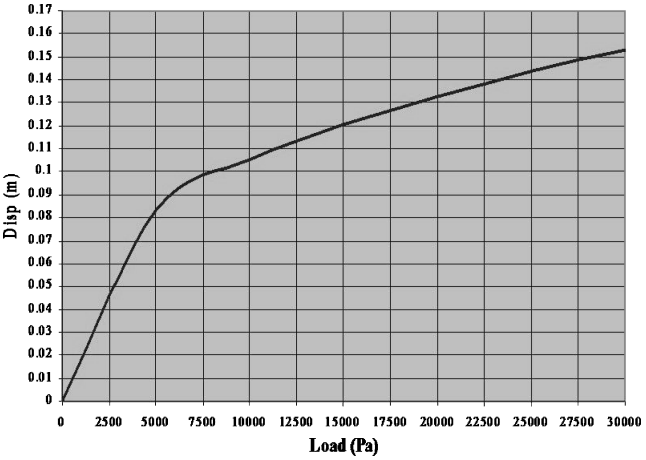

Fig. 10 Plate nonlinear response: maximum transverse displacement under increased pressure loading using shell 63.

V. Nonlinear Transient Analysis

The dynamic response of the tent to external blast loads is obtained using the transient analysis option in ANSYS. As seen from the static analysis, geometric nonlinearity plays a major role in determining the response of the structure. Therefore, a nonlinear transient analysis is conducted. An implicit approach is used, in which the Newmark method is applied for the time integration along with the Newton–Raphson method for the nonlinear solution. The Newmark method provides an unconditionally stable solution. A sparse direct solver is used for the solution due to its robustness and speed as desired in the nonlinear analysis and for large models. The full method is used for performing the nonlinear transient analysis. It is more expensive than the other two methods because it uses the full system matrices to calculate the structural response, but it takes into account geometric nonlinearity and requires no mass approximation.

A. Modeling the Blast Load

A blast refers to the fluctuation of air pressure caused by an explosion. Because of this initial finite pressure disturbance, the properties of air as a compressible gas cause the front of the disturbance to steepen as it passes through the air until it exhibits a nearly discontinuous increase in pressure, density, and temperature, resulting in a shock front. This shock front moves supersonically. The transmission of the blast wave is a nonlinear process. The air blast creates a compression wave that moves outward in all directions.[26–28]

As this pressure wave hits an obstacle in its path, part of it is transmitted and part is reflected inasmuch as it is a function of the rigidity of the reflecting surface and orientation of the surface to the wave. The reflected pressure is the pressure imposed on the structure immediately after the reflection of the pressure wave and is greater than the incident pressure. The pressure profile consists of positive and negative phases, where the positive phase is characterized by the initial sudden rise in the pressure and then decays with time until the reference pressure is reached. The negative phase is characterized by underpressure, that is, pressure below the reference pressure and then increasing to the reference pressure. The overpressure generated by the air blast surrounds the whole tent-liner system, with a time delay over the further surfaces relative to the surface facing the blast. During the field tests conducted by the U.S. Air Force Research Laboratory, pressures outside and inside the tent were measured with pressure gauges. These pressure data are used here.

The blast load is modeled as a time-varying element pressure load over the finite element model for the tent. Uniform pressure loading is assumed over each side of the tent at a given time, varying with the sides. The high overpressure causes a sudden and fast structural movement, which generates a transmitted pressure wave inside the closed structure. This internal pressure opposes the structural

movement caused by the external loading, changing the overall pressure distribution on each side. This effect is taken into account, and the resultant reduced pressure loading is applied over the structural system. Figure 11 shows the reduced pressure distribution over the sides of the tent. The reduced pressure loading applied over the back wall mainly consists of a negative pressure profile, that is, the pressure acting from inside is higher than the external loads, and this plays a significant role in the dynamics of the structure. More than 100 time steps are used to simulate the blast load over the whole structure, with the smallest time-step size being 0.5 ms.

B. Dynamic Characteristics

Structural response due to time-varying loads generally consists of displacement, stress, and strain time histories. Displacement response over each side of the shelter was computed, and the deflection at the center of each side was obtained. Figures 12–14 show displacement time histories for each side of the tent using shell 63, 181, and 41 elements, respectively. A negative displacement denotes inward movement of the side.

The first movement of the front wall, front roof, and back roof are into the tent, whereas the back wall initially moves outward. Displacement profiles for the three shell models show similar patterns. The response is accompanied by oscillations, resembling an impact response. This kind of behavior is observed for all of the sides. Peak values for shell 41 and shell 63 are almost the same for all sides, with small differences being due to the finer mesh for the shell 63 model. Shell 181 with the default drill stiffness shows a slow convergence behavior. The scaling of the drill degree of freedom and the follower load effects accelerates the convergence. This element uses the penalty approach to relate the rotational freedom to the in-plane displacements by choosing an appropriate penalty stiffness. This value can be changed by the scaling parameter provided to tune the value of the rotational stiffness. Peak values obtained using shell 181 are higher for all of the sides in comparison to the response histories obtained using the two other element types.

Figure 15 shows response snapshots. Figure 15a shows the front side movement, and Fig. 2c snapshot shows the back side movement during the time when the blast load is acting, whereas Figs. 15b and 15d show the front (Fig. 15b) and back (Fig. 15d) side response in

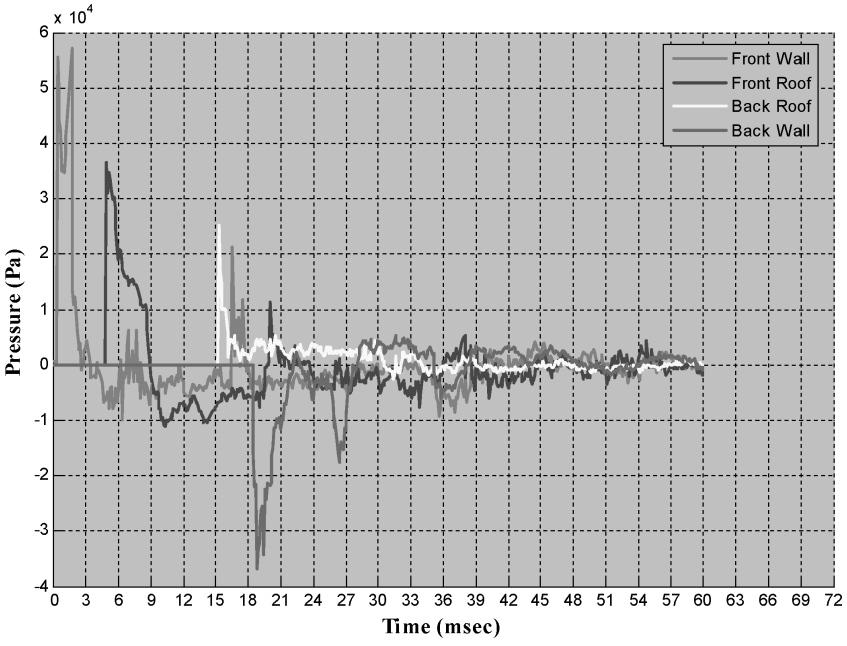

Fig. 11 Reduced-pressure loading over the tent.

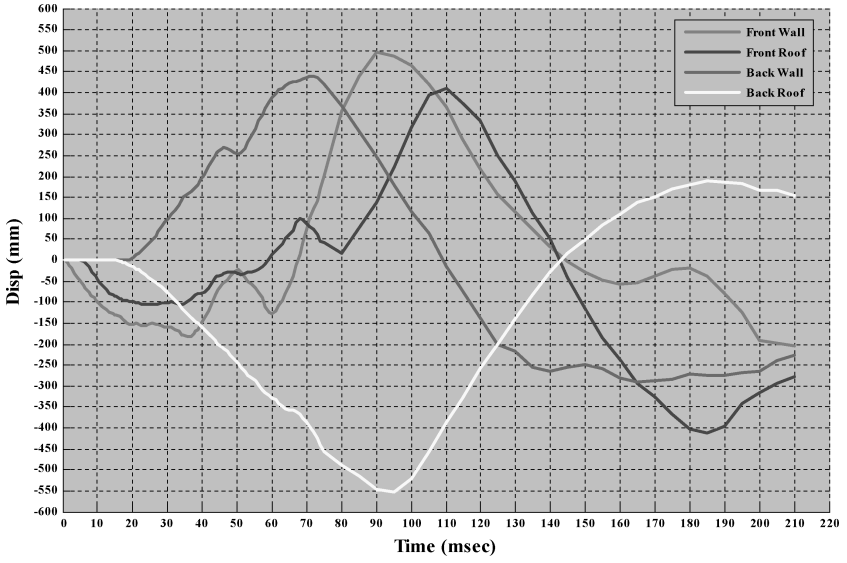

Fig. 12 Displacement vs time using shell 63 for modeling fabric skin.

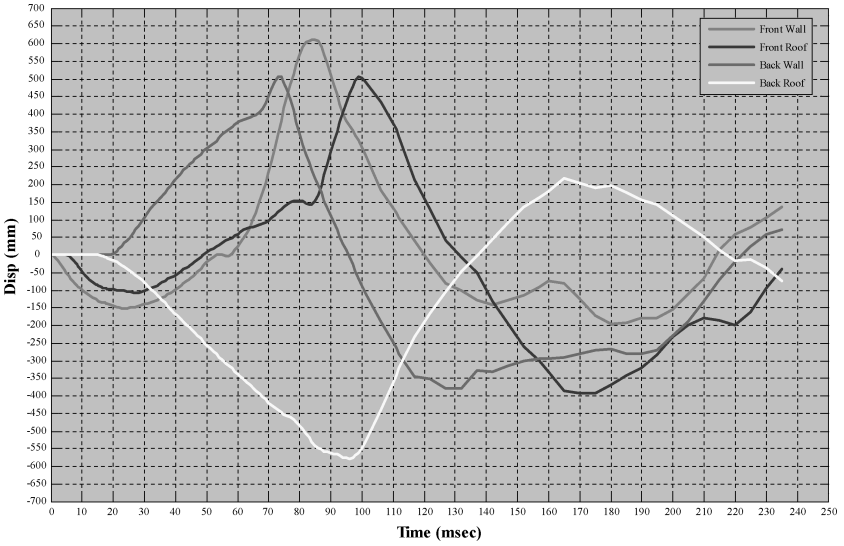

Fig. 13 Displacement vs time using shell 181 for modeling fabric skin.

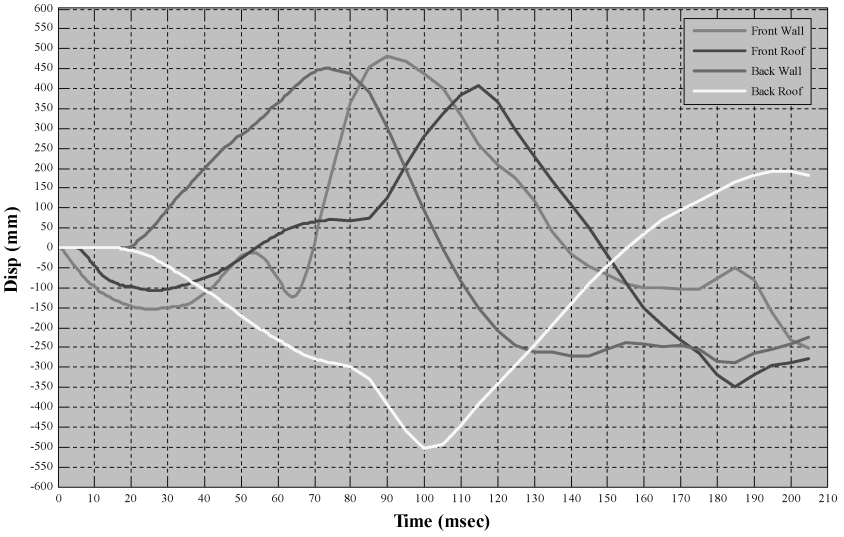

Fig. 14 Displacement vs time using shell 41 for modeling fabric skin.

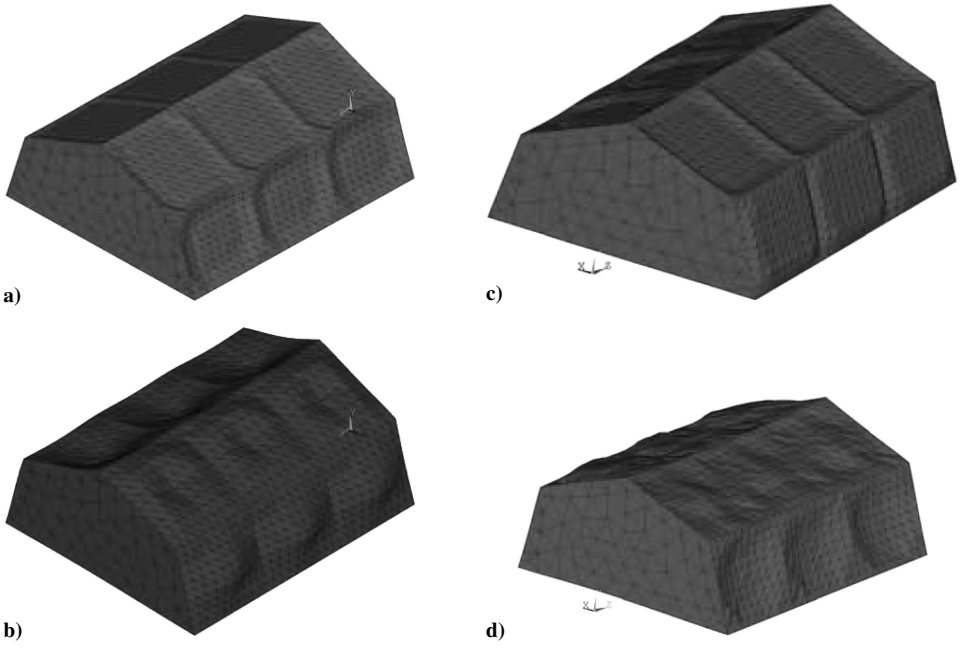

Fig. 15 Response snapshot: side movements at various times.

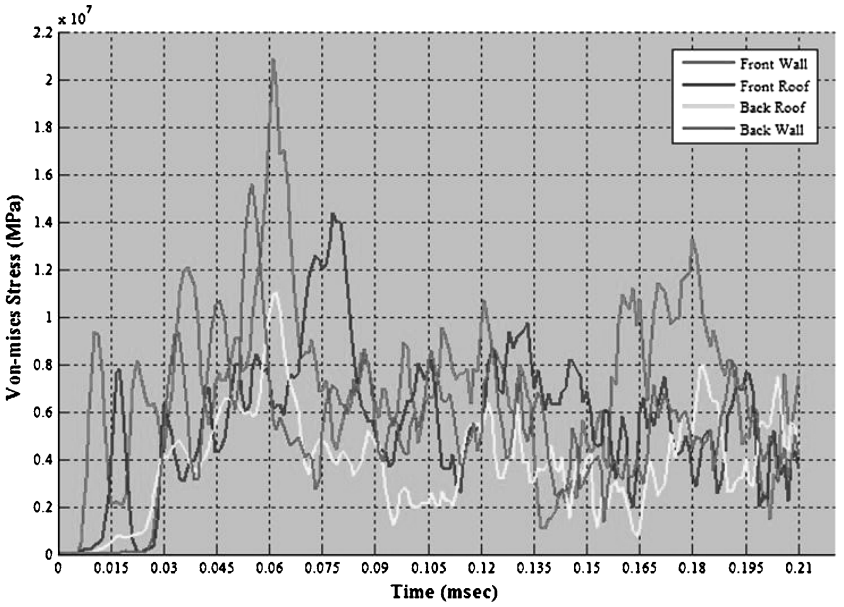

Fig. 16 Von-Mises stress vs time at center of each side of tent.

the free-vibration motion. Quantitative data (displacement vs time) are not available, but qualitative results are seen in the video file of the field tests. The deformation profiles here are similar to those seen in the video files showing the response of a tent to blast loads.

The dynamic stresses for all of the sides were computed. Figure 16 shows the Von-Mises stress vs time at the center of each side for the material model with $\rho = 9215$ kg/m^3 and $E = 250$ MPa. The stress varies significantly during the time the blast acts on the shelter and in the initial stages of the free-vibration period. A similar pattern is observed for all of the sides. The maximum stress value observed for the back wall occurs between 50 and 70 ms.

VI. Parametric Study and Analysis

Parametric studies play an important role in setting design guidelines for a given system. This consists of simulating the behavior for a number of design variations and capturing the response as a function of the design variables. A parametric study for different values of Young's modulus and density is performed.[25]

It was observed that the density of material and Young's modulus play a significant role in the response. The higher the value of E, the higher is the resistance against blast. As the value of Young's modulus is increased, the peak displacement values reduces due to stiffening. This increased stiffness leads to reduced transmitted impulse and pressure.[12] However, a disproportionate increase in stiffness leads to high stresses, which could result in failure. (Because of the lack of experimental data, damage observed in the video files could not be matched with the stress plots.) As the density was increased, the peaks displacement values were reduced.

VII. Conclusions

Finite element models for TEMPER tents were developed, and dynamic response of such a highly flexible membrane structure to blast loads was investigated using the finite element code ANSYS. Two fundamental approaches were used, one in which stress coupling was ignored (membrane model) and the other in which the stress coupling near the boundary was considered (shell model). On the computational side, responses obtained using shell 41 and shell 63 models were very similar, with shell 63 (membrane model) better from the perspective of mesh size. Shell 181 can be considered as a better model because it also includes the follower load effect. Note that the analysis was accelerated due to the combination of the follower load effect and the drill stiffness factor as compared to the shell 63 (bending and membrane combined) model where the analysis had to be abandoned as it got progressively slower. From the displacement and dynamic stress response vs time plots, it was observed that as the value of Young's modulus was increased the deflections were reduced due to stiffening, but resulted in higher stresses. Therefore, a high-modulus material should be avoided. As the mass density was increased, the peak values were reduced, showing that higher mass density results in reflecting the blast load more than transmitting it. Finally, a smaller span between the transverse frame sections reduced the peak responses (stress as well as displacement) and should be a design consideration.

Acknowledgments

This research project was sponsored by the U.S. Air Force Research Laboratory at Tyndall Air Force Base, Florida. The authors thank John Hawk, Project Monitor, for his constructive comments.

References

[1]Jenkins, C. H. M. (ed.), *Gossamer Spacecraft: Membrane and Inflatable Structures Technology for Space Applications*, AIAA, Reston, VA, 2001.

[2]Hammons, M. I., "Antiterrorism/Force Protection Criteria Validation Test," Force Protection Branch, Airbase Technologies Div., U.S. Air Force Research Lab., Tyndall AFB, FL, March 2000.

[3]Donahue, K. L., "Chemical and Biological Barrier Materials for Collective Protection Shelters," U.S. Air Force Research Lab., Tyndall AFB, FL, 2003, http://www.natick.army.mil/soldier/jocotas/ColPro_Papers/Donahue.pdf.

[4]http://www.army-technology.com/contractors/field/index.html.

[5]Mohan, P., and Kapania, R. K., "Static, Free Vibration and Thermal Analysis of Composite Plates and Shells Using a Flat Triangular Shell Element," *Computational Mechanics*, Vol. 17, No. 5, 1996, pp. 343–357.

[6]Carradine, D. M., and Plaut, R. H., "Arch-Supported Membrane Shelters Under Wind and Snow Loading," *International Journal of Space Structures*, Vol. 13, No. 4, 1998, pp. 197–202.

[7]Porter, J. R., Hawk, J. R., and Hammons, M. I., "Survivability of Collective Protection Systems Subjected to Air Blast Loads," U.S. Air Force Research Lab., Tyndall AFB, FL, 2003.

[8]Turkmen, H. S., "Structural Response of Isotropic Plates Subject to Blast Loading," *Advances in Computational Structural Mechanics*, Civil-Comp Press, Edinburgh, 1998, pp. 101–107.

[9]Gupta, A. D., Gregory, F. H., Bitting, R. L., and Bhattacharya, S., "Dynamic Analysis of an Explosively Loaded Hinged Rectangular Plate," *Computers and Structures*, Vol. 26, No. 1–2, 1987, pp. 339–344.

[10]Koh, C. G., Ang, K. K., and Chan, P. F., "Dynamic Analysis of Shell Structures with Application to Blast Resistant Doors," *Shock and Vibration*, Vol. 10, No. 4, 2003, pp. 269–279.

[11]Louca, L. A., and Pan, Y. G., "Response of Stiffened and Unstiffened Plates Subjected to Blast Loading," *Engineering Structures*, Vol. 20, No. 12, 1998, pp. 1079–1086.

[12]Scherbatiuk, K. D., "Effect of a Flexural Membrane on Blast Transmission and Mitigation," *Proceedings of Response of Structures to Extreme Loading Conference*, Toronto, 2003.

[13]Crawford, J. E., and Morrill, K. B., "Development of a Lightweight, Portable Airblast Barrier," *MABS16 Conference*, 2000, http://www.kcse.com/pdfs/KCSE_MABS_Paper_f.pdf.

[14]Zhu, L., "Transient Deformation Modes of Square Plate Subjected to Explosive Loading," *International Journal of Solids and Structures*, Vol. 33, No. 3, 1996, pp. 301–314.

[15]Turkmen, H. S., "Structural Response of Laminated Composite Shells Subjected to Blast Loading: Comparison of Experimental and Theoretical Methods," *Journal of Sound and Vibration*, Vol. 249, No. 4, 2002, pp. 663–678.

[16]Niyogi, A. G., Laha, M. K., and Sinha, P. K., "Finite Element Vibration Analysis of Laminated Composite Folded Plate Structures," *Shock and Vibration*, Vol. 6, No. 5–6, 1999, pp. 273–283.

[17]Chen, J., Dawe, D. J., and Wang, S., "Nonlinear Transient Analysis of Rectangular Composite Laminated Plates," *Composite Structures*, Vol. 49, No. 2, 2000, pp. 129–139.

[18]Jenkins, C. H., and Leonard, J. W., "Nonlinear Dynamic Response of Membranes: State of the Art," *Applied Mechanics Reviews*, Vol. 44, No. 7, 1991, pp. 319–328.

[19]Smalley, K. B., Tinker, M. L., and Taylor, W. S., "Structural Modeling of a Five-Meter Thin-Film Inflatable Antenna/Concentrator," *Journal of Spacecraft and Rockets*, Vol. 40, No. 1, 2003, pp. 27–29.

[20]Zienkiewicz, O. C., *The Finite Element Method in Engineering Science*, McGraw–Hill, London, 1971.

[21]*ANSYS Release 8.0 Documentation*, 2004.

[22]Lee, P. S., and Bathe, K. J., "On the Asymptotic Behavior of Shell Structures and the Evaluation in Finite Element Solutions," *Computers and Structures*, Vol. 80, No. 3–4, 2002, pp. 235–255.

[23]Chappelle, D., and Bathe, K. J., *The Finite Element Analysis of Shells—Fundamentals*, Springer-Verlag, Heidelberg, Germany, 2003.

[24]Knight, N. F., Jr., "Raasch Challenge for Shell Elements," *AIAA Journal*, Vol. 35, No. 2, 1997, pp. 375–381.

[25]Kapoor, H., Chun, S., Kapania, R. K., Motley, M. R., and Plaut, R. H., "Structural Response of Large Flexible, Deployable Shelters to Blast Loads," *46th AIAA/ASME/ASCE/AHS/ASC Structures, Structural Dynamics, and Materials Conference*, AIAA, Reston, 2005, pp. 2009–2030.

[26]Baker, W. E., *Explosions in Air*, Univ. of Texas Press, Austin, TX, 1973.

[27]Smith, P. D., and Hetherington, J. G., *Blast and Ballistic Loading of Structures*, Butterworth–Heinemann, Oxford, 1994.

[28]Beshara, F. B. A., "Modeling of Blast Loading on Aboveground Structures—I. General Phenomenology and External Blast," *Computers and Structures*, Vol. 51, No. 5, 1994, pp. 585–596.

A. Palazotto
Associate Editor